

Load-Balancing Algorithm for Multiple Gateways in Fog-Based Internet of Things

Fatemeh Banaie, *Student Member, IEEE*, Mohammad Hossein Yaghmaee^{ID}, *Senior Member, IEEE*, Seyed Amin Hosseini^{ID}, and Farzad Tashtarian

Abstract—This article investigates the performance of multicriteria-based load-balancing scheme among gateways in fog-assisted Internet of Things (IoT). We employ a queueing model of the IoT system to calculate the latency of data streams from the IoT devices to the applications. However, a gateway node may easily become congested since all the traffic to IP networks are directed toward the gateway. A congested point can affect system performance and may cause reliability problems in the system. Thus, we employ multiple gateways to alleviate the performance degradation of the network, along with a multicriteria decision-making (MCDM)-based load-balancing policy among the gateways to achieve a global load fairness. The proposed model is evaluated in single-hop IPv6 over low-power wireless personal area networks (6LoWPANs). The evaluation results show the effectiveness of the proposed load-balancing model in providing fast and reliable responses to user queries.

Index Terms—IPv6 over low-power wireless personal area network (6LoWPAN), fog-based Internet of Things (IoT), hybrid proxy, load balancing, multicriteria decision making (MCDM).

20

I. INTRODUCTION

THE Internet of Things (IoT) has been developed as an intriguing paradigm that describes the connections of smart objects and devices over IP networks with the support of modern communication techniques [1], [2]. The IoT enables things to observe and sense the environment states, to make coordinated decisions in various sensing service applications, such as smart transportation, smart healthcare, home automation, and smart city. In order to realize the full benefits of the IoT, it is necessary to provide the new innovative networking technologies and communication schemes, which allows IPv6 communications over low-power and lossy networks (LLNs) such as wireless sensor networks (WSNs) [3]–[5].

To this end, the Internet Engineering Task Force (IETF) has developed some standardized communications protocols, such as the IPv6 over low-power wireless personal area networks (6LoWPANs) [6], the routing protocol for low power and lossy network (RPL) [7], and the constrained application protocol (CoAP) [8] to tackle the technical challenges of the

existing protocol's overhead against the limitations of the sensing devices in the terms of constrained energy, memory, and computational resources [9]. However, providing sufficient computing resources to process and store the huge amount of generated data by the distributed IoT devices is necessary to alleviate the traffic load in the network and minimize the latency of IoT devices [11].

Owing to the large volumes of high-velocity streams of data, a specialized platform is employed to process and store the big data generated from the distributed IoT devices. The platform can provide flexible and efficient computing resources by connecting to a remote cloud backend [12], [13]. Such an architecture can offer localized services by leveraging the processing and storage resources of the cloud on the edge of the network, known as *fog computing*. Specifically, in-network computation is provided through edge devices (e.g., gateways located on the fog nodes) by initially processing the collected data from the distributed sensors and transmitting the refined data toward the requested host. This is necessary to facilitate the service management and real-time processing of data from a wide variety of IoT devices [14]. However, transmitting the generated data from the IoT devices to the gateways may consume high bandwidth and energy of the IoT devices. Besides, it increases the latency of data processing in the network, which makes it intolerable for many delay-sensitive applications [15].

To accommodate performance issues, content caching in the application layer is proposed to speed up the delivery rate of the processing data and solve the energy efficiency problem. Therefore, the sensed data will be sent to the gateway by the IoT devices and clients can access the sensed data from the gateway rather than the IoT device. However, all of this generated traffic from low-power wireless personal area networks (LoWPANs) should pass through the gateway, which may easily become congested bottleneck and cause reliability problems [16]. Multiple gateways can be employed to relieve this issue and provide efficient connectivity within the IoT network.

Two adjacent gateways may be located close to each other, thus, having overlapped coverage areas. Consequently, each IoT device may be associated with one or more gateway(s) of the edge nodes. In this case, the traffic loads among the gateways may be unbalanced due to the absence of the proper load-balancing scheme. The overloaded gateways will become the bottleneck of the system, thus causing longer communications latency of data streams in the network. Over several research works in literature, applications workload is assigned

AQ1

Manuscript received September 26, 2019; revised January 3, 2020 and February 12, 2020; accepted March 9, 2020. (Corresponding author: Seyed Amin Hosseini.)

Fatemeh Banaie, Mohammad Hossein Yaghmaee, and Seyed Amin Hosseini are with the Department of Computer Engineering, Ferdowsi University of Mashhad, Mashhad 9177948974, Iran

AQ2

Farzad Tashtarian is with the Mashhad Branch, Islamic Azad University, Mashhad, Iran.

Digital Object Identifier 10.1109/JIOT.2020.2982305

to each gateway according to the required computing resource in a hierarchical cloudlet network in [17]. Specifically, an application-aware load-balancing scheme is applied in [18] to select the destination gateways for different types of user requests and the amount of computing resources allocated for each application in each cloudlet. However, assigning all workloads of the application to a specific gateway would incur the recaching problem among gateways in a dynamic IoT environment. To solve the problem, a multicriteria decision-making (MCDM)-based load-balancing technique can be employed to alleviate the network latency by efficiently associating the task requests among the overlapping gateways.

In this article, we present an analytical model to evaluate the performance of traffic load balancing in a multiple gateway-enabled IoT system. The proposed load-balancing model in this article is twofold. First, a queuing network problem is solved to evaluate the latency of task executing in the network. After modeling, an MCDM-based load-balancing scheme is used to balance the traffic loads among the gateways to achieve a global load fairness and reduced latency of service processing in the IoT system. The main contributions and key results of this article are summarized as follows.

- 1) We present a model-driven and analytical approach to evaluate the performance of a load-balanced multigateway-enabled IoT system. To the best of our knowledge, this is the first study that considers the $M/G/1$ system with a multiple vacation model for evaluating the network latency in load balancing the traffic loads among gateways. In this model, the busy period of the controller for processing the task requests of other gateways induce vacations for each of the other gateways. The works of literature consider a simple $M/M/1$ model for evaluating the network delay [16]–[19]. However, despite the Poisson process provide a good approximation of the arrival rate in real systems [20], exponential distribution may not provide a general estimation of the real-world scenarios. Considering more general queuing models can increase the effectiveness of the evaluation model for real-world applications.
- 2) We formulate the problem of workload allocation into the gateways as a multiobjective optimization problem in the form of a mixed-integer linear programming (MILP). The proposed MILP model tries to balance the network load by minimizing the maximum loads of the gateways. Since this problem is NP-complete, we apply an MCMD method for gateway selection by taking into account their load changes over time in order to deal with the high time complexity issue of the MILP model, particularly in large-scale scenarios. The analytical hierarchy process (AHP) is one of the most popular MCDM method that is being used in complex decision-making processes due to its simplicity and consistency [21]–[23]. It is an effective method in the decision-making problem (e.g., load management problem) that selects the most suitable gateway by evaluating the candidate gateways.
- 3) We deploy the IPv6 protocol stack over sensor devices and integrate the IoT devices with multiple gateways

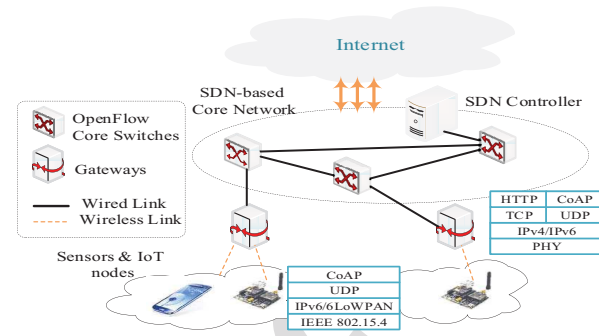


Fig. 1. Example scenario of IoT sensing system.

load-balancing method to make the evaluation closer to the real-world models.

The remainder of this article is organized as follows. In Section II, we briefly describe the system model used in this article. In Section III, the proposed analytical load-balancing scheme is described in detail. In Section IV, we demonstrate and discuss the evaluation results, followed by the conclusion in Section V.

II. SYSTEM MODEL

This article considers a multigateway-based 6LoWPAN architecture that supports the MCDM-based load-balancing method to balance the traffic loads among the gateways. In this architecture, which is schematically shown in Fig. 1, all sensor nodes access the Internet through the gateways. The gateway deployment leverages the edge IoT architecture in which gateways are border entities in the networks and handle ingress and egress data traffic. In addition, a software-defined networking (SDN)-based core is used to connect the gateways to the Internet. Gateway nodes are connected to the OpenFlow-enabled switches that separate out the control functions from data forwarding functions. The SDN controller manages the gateway nodes via the OpenFlow-based switches that monitor the traffic at the data plane [24]. It also has a load-balancing function to associate the user load to the gateways in a fairly manner.

The sensor nodes keep measuring the environmental parameters, e.g., noise-level measurement, and send the measured data to the gateways using CoAP POST methods in a confirmable (CON) mode. Since the CoAP protocol utilizes UDP in the transport layer, it supports optional reliability by defining two modes of messages: 1) CON and 2) non-confirmable (NON). To ensure reliable communication, the messages are retransmitted with exponential timeouts until the receiver acknowledges the reception of data or it reaches to the maximum number of retransmissions.

A Web application accesses the measured data via a gateway/proxy with a cache deployed on it to allow some of the user queries to be served from the cache. However, the IoT data are transient [25], i.e., it has a lifetime and expires after this time period. Therefore, a caching policy is required to keep the cached data up-to-date in the proxy. We employed a CoAP proxy to leverage the functionalities offered by the proxy in decoupling the applications from physical sensors and

186 devices. A CoAP proxy usually operates in different operational modes of *forward proxy* and *reverse proxy*. In the former case, proxy obtains the sensed data by sending CoAP GET methods, while in the latter case, a periodical transmission of the sensed data is used by the IoT nodes. *Hybrid proxy* can leverage the benefits of both forward and reverse proxies [8]. In this model, a reverse proxy with occasional forward queries serves as a gateway between applications and sensor nodes.

194 Upon receiving a request, the cache decides whether to 195 retrieve the fresh sensing data from the sensors using the CoAP 196 GET method (in piggybacked CON mode) or to use the cached 197 sensing data. Let $\mathcal{G} = \{1, \dots, m\}$ denotes a set of gateways in 198 the system and λ be the aggregated task request arrival rate to 199 the system. Thus

$$200 \quad \lambda = \sum_{g=1}^m \lambda_g, \quad g \in \mathcal{G} = \{1, \dots, m\} \quad (1)$$

201 where λ_g is the arrival rate to each gateway $g \in \mathcal{G}$ and m is 202 the number of gateways. If we assume that IoT nodes send 203 the data in exponentially distributed time periods with mean 204 $\bar{T}_s = 1/\lambda_s = 60$ s, the probability that the user query finds 205 the outdated records (ORs) in different gateways is denoted 206 by [29]

$$207 \quad P_{\text{OR},g} = \int_{x=\bar{T}_s}^{\infty} P\{A_g < A_s | A_g = x\} dB(x) \\ 208 \quad = \frac{\lambda_g}{\lambda_s + \lambda_g} e^{-(\lambda_g + \lambda_s)\bar{T}_s}, \quad g \in \{1..m\}. \quad (2)$$

209 The above expression calculates the probability that interarrival 210 times between the user requests is smaller than the cache 211 update intervals (i.e., $\text{Prob}[A_g < A_s]$), consequently it shows 212 the probability of data requests that should be forwarded to 213 the IoT devices. A_g and A_s are the Laplace–Stieltjes transform 214 form (LST) of the interarrival time of the user requests to the 215 gateway $g \in \mathcal{G}$ and the refresh messages of the sensor nodes, 216 respectively. As Poisson interarrival times are exponential random 217 variables, they are typically exponentially distributed and 218 the LST of number of arriving messages can be defined as

$$219 \quad A_j^*(s) = \int_0^{\infty} e^{-sx} \lambda_j e^{-\lambda_j x} dx = \frac{\lambda_j}{\lambda_j + s}, \quad j \in \{g, s\}. \quad (3)$$

220 Thus, the required refreshment messages are sent with the 221 rate $\lambda_{get,g} = \lambda_g \times P_{\text{OR},g}$.

222 III. TRAFFIC LOAD BALANCING AMONG GATEWAYS

223 A. Problem Statement

224 There are often several overlapping gateways in the IoT 225 domain running over IEEE802.15.4/6LoWPAN, which play a 226 significant role in packet delivery as a relay point and end- 227 devices. The generated traffic in 6LoWPAN is directed to 228 the Internet via the gateways. To this end, a multigateway- 229 based architecture can provide significant benefits in terms 230 of network capacity and reliability. Normally, an SDN server 231 would select the nearest local gateway with more computa- 232 tional resources for task association. However, this may lead 233 to the imbalanced traffic load among gateways, so that some

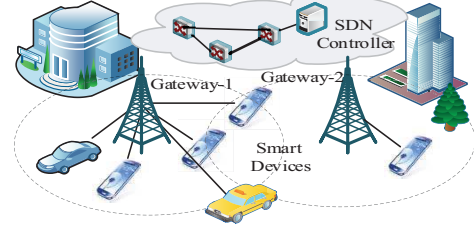


Fig. 2. Illustration of unbalanced traffic loads among gateways.

gateways suffer from heavy loads while the others are lightly loaded.

The heavily loaded gateways may confront the increased cache miss rate that will rise the need for retrieving the fresh data from the IoT devices. Apart from the energy exhaustion of the nodes that are close to these gateways, it may incur a higher delay beside the longer processing queues, which necessitates applying a workload-balancing scheme among the overlapping gateways.

Fig. 2 depicts a scenario of unbalanced traffic among gateways in a smart city application. Let us consider a smart city system in which the streets and buildings are equipped with smart devices and sensors. These smart devices sense the environmental parameters and send them to the nearest gateway that is available for them. Suppose in a special holiday, a large number of retrieval requests for finding the available parking spot, location of special places, traffic monitoring, weather conditions, etc., are sent toward these devices. Consequently, each device may need to transmit a large amount of data to these requests, which may result in increased delay of network and exhaust the energy supplies of the resources. In order to efficiently deliver the sensed data, the gateways cache their data periodically and respond to the requests on behalf of the devices. Normally, the gateways at the main streets or crowded places receive the most client retrieval requests that may lead to the improper load balancing and congestion on links nearby them. The unbalanced traffic loads may significantly increase the average delay of the network and disable the efficient data transmitting in the smart city system.

To this end, we leverage a load-balancing strategy of multiple gateways based on the SDN-based core network. In this method, the controller obtains an evenly balanced server load by considering the changing features of the network, such as resource loads and available resources. The SDN controller is a logical entity that implements the network policy, such as traffic scheduling and load management [26]. This solution can achieve a global load fairness and reduced latency of service processing in the IoT system. Furthermore, combining the load-balancing technology with the resource caching method provides reduced energy consumption for the IoT devices.

B. Problem Formulation

To formulate the problem, we have defined L as the total load of a set of overlapping gateways, $\mathcal{G} = \{g_1, g_2, \dots, g_m\}$, where m is the number of gateways in each overlapping area. γ_t represents the load factor of each individual task, and the residual load capacity of each gateway is denoted by $L_{\text{res},g}$.

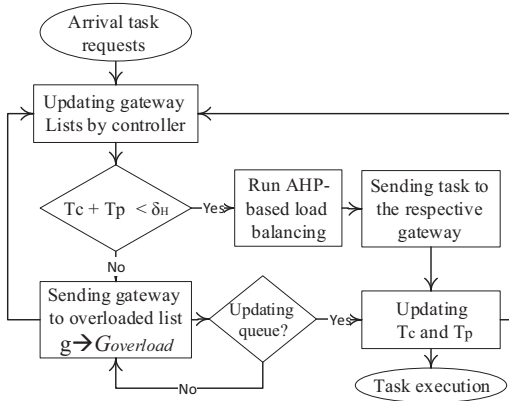


Fig. 3. MCDM-based load-balancing scheme.

280 respectively. The problem can be formulated as

$$\begin{aligned}
 \min \quad & \alpha L + \beta \sum_t \sum_g B_{t,g} \\
 \text{s.t.} \quad & \text{C1: } \sum_{t \in \text{tasks}} B_{t,g} \gamma_t < L \quad \forall g \in \text{gateways} \\
 & \text{C2: } \sum_{t \in \text{tasks}} B_{t,g} \gamma_t < L_{\text{res},g} \quad \forall g \in \text{gateways} \\
 & \text{C3: } \sum_{g \in \text{gateways}} B_{t,g} \leq 1 \quad \forall t \in \text{tasks} \\
 \text{Var.} \quad & L_g \geq 0, \quad B_{t,g} \in \{0, 1\}.
 \end{aligned} \tag{4}$$

286 $B_{t,g}$ is a binary variable indicating whether the task t
 287 is assigned to the gateway g (i.e., $B_{t,g} = 1$) or not (i.e.,
 288 $B_{t,g} = 0$). α and β represent the importance of the load factor
 289 of gateways and the number of assigned tasks in the objective
 290 function, respectively. Constraints C1 and C2 ensure that the
 291 assigned load to each gateway must be less than the resid-
 292 ual load capacity of the gateways. Constraint C3 imposes that
 293 each task can be allocated to exactly one gateway.

294 *Theorem 1:* The problem of fairly assigning tasks to a set
 295 of overlapping gateways is NP-complete.

296 *Proof:* Let us consider m gateways where each of which
 297 can process at most $L_{\text{res},g}$, $g = 1 \dots m$, amount of work-
 298 loads. Moreover, without loss of generality, we define a set of
 299 requesting tasks with different weights w_g as the load factor
 300 of the task and the value v_g as the perceived gain by the users.
 301 The goal is to assign the maximum number of tasks (e.g., max-
 302 imum value) to the gateways given the maximal load capacity
 303 of the gateways. Thus, the problem is reduced in polynomial
 304 time to the known 0-1 multiple Knapsack problem [27]. Since
 305 the 0-1 multiple Knapsack problem is known as NP-complete,
 306 we can conclude that the addressed problem is NP-complete. ■

307 C. Heuristic Algorithm

308 The proposed MILP model is in the form of an NP-complete
 309 problem, thus we use the AHP algorithm to tackle the time
 310 complexity of the problem. To investigate the performance of
 311 multigateway systems, it is essential to calculate the overall
 312 latency of the network. The overall latency of the data streams
 313 (T_{tot}) consists of the *transmission delay* (T_t) toward gateways

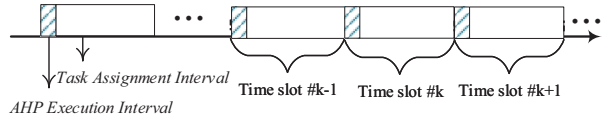


Fig. 4. Time slots in AHP method.

and the *processing delay* (T_p) by the respective gateway. Thus,
 314 we have

$$T_{\text{tot},g} = T_{t,g} + T_{p,g}. \tag{5}$$

The former delay can be neglected if the cached data are
 317 used instead of the retrieving data from sensor nodes.
 318 AQ3

The local controller consists of two components: 1) traffic
 319 monitoring module (TMM) and 2) load optimization module
 320 (LOM). The TMM is responsible for the collection, analysis,
 321 and reporting of the traffic load on each gateway. It per-
 322 forms the operation by separating the gateway's traffic loads
 323 and analyzing the latency of gateways. Then, it assigns them
 324 into three different lists named *over-loaded*, *under-loaded*, and
 325 *normal-load* gateways
 326

$$L_c = \begin{cases} g \rightarrow \mathcal{G}_{\text{Overload}} & T_{\text{tot},g} > \delta_H \\ g \rightarrow \mathcal{G}_{\text{Normalload}} & \delta_M \leq T_{\text{tot},g} \leq \delta_H \\ g \rightarrow \mathcal{G}_{\text{Underload}} & T_{\text{tot},g} < \delta_M \end{cases} \tag{6}$$

where δ_H and δ_M are the upper and lower thresholds of
 328 the queuing latency, respectively. These parameters can be
 329 adjusted according to the network specifications. TMM will
 330 also collaborate with LOM in the enhancing gateway's traf-
 331 fic loads, with the intent to ensure fairness and reduce the
 332 network latency and the energy consumption of sensor nodes.
 333 After classifying the gateway lists regarding queue latency,
 334 LOM is responsible for assigning tasks at each time slot τ .
 335 In fact, each time slot is divided into two intervals. The first
 336 interval is allocated for running the AHP algorithm and in the
 337 second interval, the arriving tasks are allocated to the selected
 338 gateway until the end of τ (Fig. 4). This will prevent the unnec-
 339 essary service delay, which is essential in delay-sensitive IoT
 340 applications.
 341

Thus, the load-balancing mechanism consists of three
 342 iterative process.
 343

Step 1: TMM monitors the traffic load of the associated
 344 gateways and accordingly assign them into three
 345 different lists named as over-loaded, under-loaded,
 346 and normal-load.
 347

Step 2: LOM applies the AHP decision-making method
 348 for the overlapping gateways in *normal-loaded* and
 349 *under-loaded* lists to find the best suitable server
 350 for incoming tasks.
 351

Step 3: After assigning the tasks to each gateway, the load
 352 of the gateway is updated by the monitoring module
 353 of the controller. The server load may also change
 354 in task departure time.
 355

Thus, in order to calculate the task processing latency of
 356 the gateways, at first, we will focus on the transmission and
 357 processing delay of each gateway in the network. The notation
 358 for the most important parameters is shown in Table I.
 359

TABLE I
IMPORTANT PARAMETER NOTATION

Parameter	Description
m	Number of gateways
λ	Incoming task rate
λ_s	The rate of update messages sent by IoT nodes
λ_g	The arrival rate of gateway g
$P_{OR,g}$	The probability of cache miss rate in g
T_{tot}	overall latency of data streams
T_t	transmission delay
T_p	Processing delay
B_g	Service time of gateway g
V_g	Vacation duration of gateway g
τ_g	Probability of taking phase $K + 1$

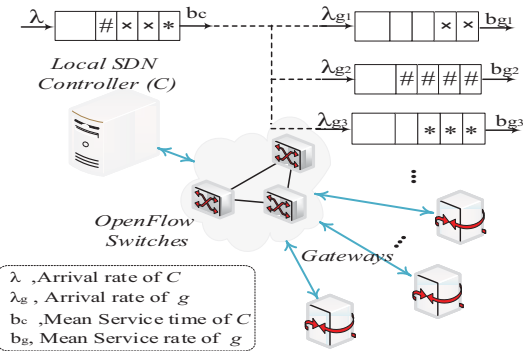


Fig. 5. Queueing model of gateway deployment.

360 D. Delay Analysis of Network

361 In this section, we suppose that the system consists of m
362 homogeneous gateways, which independently render service
363 to the jobs in a nonpreemptive fashion according to the FCFS
364 discipline. The SDN controller acts as an $M/D/1$ queueing
365 system which indicates that the interarrival time of requests
366 exponentially distributed with a rate of $1/(\lambda = \sum_{g=1}^m \lambda_g)$,
367 while task service times are deterministic and it depends on
368 the resource capacity of the controller. When the controller
369 receives a new job request, it processes the requests and
370 forwards it to the respective gateway, as shown in Fig. 5.

371 Each gateway is modeled as an $M/G/1$ queuing system with
372 multiple vacations model [30]. The vacation queueing models
373 are an extension of the classical queueing theory in which the
374 server becomes unavailable (performing nonqueueing jobs) for
375 some potentially random period of time. The vacation process
376 could be characterized by three aspects: 1) vacation start-up
377 rule; 2) vacation termination rule; and 3) vacation duration
378 distribution [31]. These models make queueing systems more
379 realistic and flexible for real-world scenarios by allowing the
380 server to perform nonqueueing jobs. In this case, the vacation
381 model is applied for enabling to calculate the request pro-
382 cessing latency induced by the controller. In other words, the
383 latency of task processing by the controller for each stream
384 is obtained in the gateway side. Because the controller is not
385 able to classify the streams due to the dynamic distributions of
386 tasks and resources. Thus, the busy period of the controller for
387 processing the task requests of other gateways induces a vaca-
388 tion for each gateway. In vacation systems, the server goes on
389 vacation for some potentially random period of time. When the
390 server returns from a vacation and its buffer is not empty, the

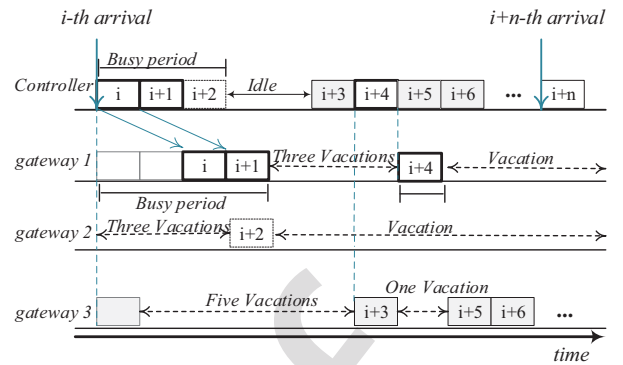


Fig. 6. System behavior with three gateways.

service period starts. As shown in Fig. 6, when the controller 391
392 serves a request belonging to a gateway g , other gateways start 393
394 a vacation if their queue is empty. 395

The task request arrival to each gateway, $g \in \mathcal{G} = \{1 \dots m\}$, 396 follows the Poisson process with an arrival rate of λ_g and 397 has independent and identically distributed service time with 398 a mean value of b_g . Without loss of generality, we supposed 399 that the service time of all gateways are the same 400 and is $B_G(s) = B_g(s)$, $g \in \{1, \dots, m\}$. Upon completion 401 of a service if there are no tasks in the queue, the server 402 takes vacation consisting of K -phases with each phase has 403 time duration $V_{g,1}, V_{g,2}, \dots, V_{g,K}$ with the distribution func- 404 tions $V_{g,k}(x) = B_c(x)$, $g \in \{1 \dots m\}$ and $k \in \{1 \dots K\}$. Let 405 $\tau_g = (1 - [\lambda_g/\lambda])$ be the probability that the server takes the 406 phase $k + 1$ after completion of the phase k . Therefore, the 407 server will take a vacation with the probability τ_g , and it will 408 take a service period with the probability $(1 - \tau_g)$. This means 409 that taking a 1-phase vacation period could be happened with 410 the probability of $\tau \times (1 - \tau)$, and a 2-phase vacation duration 411 has the probability of $\tau \times \tau \times (1 - \tau)$. Hence, the vacation 412 period in the system is defined as 413

$$\begin{aligned} V_g &= V_{g,1} \quad \text{with probability } \tau_g(1 - \tau_g) \\ &= V_{g,1} + V_{g,2} \quad \text{with probability } \tau_g^2(1 - \tau_g) \\ &\dots \\ &= V_{g,1} + \dots + V_{g,K-1} \quad \text{with probability } \tau_g^{K-1}(1 - \tau_g) \\ &= V_{g,1} + \dots + V_{g,K} \quad \text{with probability } \tau_g^K(1 - \tau_g). \end{aligned} \quad (7) \quad 414 \quad 415 \quad 416$$

Since all vacation phases have the same distribution function, 417 i.e., $V_{g,j}(x) = B_c(x)$ for all $j \in \{1, K\}$, thus, the LST of 418 V_g is 419

$$V_g^*(x) = \sum_{j=1}^K (V_{g,j}^*(x) \tau_g^j) (1 - \tau_g) = \sum_{j=1}^K (B_c^*(x) \tau_g^j) (1 - \tau_g) \quad 420 \quad 421 \quad (8) \quad 422$$

where $V_{g,j}^*(x) = \sum_{i=1}^j V_{g,i}^*$. Assume that all $V_{g,j}, j \in \{1 \dots K\}$ 423 are mutually independent. In this case, the conditional LSTs 424 of $V_{g,j}$ can be expressed as 425

$$\sum_{j=1}^K V_{g,j}^*(x) = (V_g^*(x))^K. \quad (9) \quad 425$$

426 Thus, we have

$$427 \quad V_g^*(x) = \sum_{k=1}^K (B_c^*(x)\tau_g)^k (1 - \tau_g). \quad (10)$$

428 To model the system, a set of Markov point $\{L_n, n = 1, 2, \dots\}$ is considered at which either a vacation is ended
429 or a service is ended, where L_n is the number of task requests
430 in the system immediately after the n th Markov point. Let Θ_n
431 be the state of the gateway at the n th Markov point denoted
432 by

$$434 \quad \Theta_n \triangleq \begin{cases} 0, & \text{end of a vacation} \\ 1, & \text{end of a service.} \end{cases} \quad (11)$$

435 The steady-state joint distributions of the number of tasks
436 in g are defined by

$$437 \quad q_{g,k} \triangleq \lim_{n \rightarrow \infty} \text{Prob}[\Theta_n = 0, L_n = k], \quad k = 0, 1, 2, \dots \quad (12)$$

$$438 \quad \pi_{g,k} \triangleq \lim_{n \rightarrow \infty} \text{Prob}[\Theta_n = 1, L_n = k], \quad k = 0, 1, 2, \dots \quad (13)$$

439 and the corresponding generating functions are defined by

$$440 \quad Q_g(z) \triangleq \sum_{k=0}^{\infty} q_{g,k} z^k \quad (14)$$

$$441 \quad \Pi_g(z) \triangleq \sum_{k=0}^{\infty} \pi_{g,k} z^k. \quad (15)$$

442 The model is governed by the following balance equations:

$$443 \quad q_{g,k} = (q_{g,0} + \pi_{g,0})f_{g,k} \quad k \geq 0 \quad (16)$$

$$444 \quad \pi_{g,k} = \sum_{j=1}^{k+1} (q_{g,j} + \pi_{g,j})a_{g,k-j+1} \quad k \geq 0 \quad (17)$$

$$445 \quad \sum_{k=0}^{\infty} q_{g,k} + \sum_{k=0}^{\infty} \pi_{g,k} = 1 \quad (18)$$

446 where $f_{g,k}$ is the probability that there are k arrivals for g
447 during a vacation time that its PGF is defined as

$$448 \quad F_g(z) = \sum_{k=0}^{\infty} f_{g,k} z^k = \int_0^{\infty} e^{-\lambda_g(1-z)x} dV_g(x) \\ 449 \quad = V_g^*(\lambda_g - \lambda_g z). \quad (19)$$

450 Similarly, $a_{g,k}$ is the probability that k tasks arrive for g
451 during a service time with the PGF of

$$452 \quad A_g(z) = \sum_{k=0}^{\infty} a_{g,k} z^k \\ 453 \quad = \int_0^{\infty} e^{-\lambda_g(1-z)x} dB_G(x) = B_G^*(\lambda_g - \lambda_g z). \quad (20)$$

454 Thus, we can write these equations as

$$455 \quad Q_g(z) = (q_{g,0} + \pi_{g,0})V_g^*(\lambda_g - \lambda_g z) \quad (21)$$

$$456 \quad \Pi_g(z) = [Q_g(z) + \Pi_g(z) - (q_{g,0} + \pi_{g,0})] \frac{B_G^*(\lambda_g - \lambda_g z)}{z} \quad (22)$$

$$457 \quad Q_g(1) + \Pi_g(1) = 1. \quad (23)$$

From (22) and (23), we get

$$459 \quad \Pi_g(z) = \frac{(q_{g,0} + \pi_{g,0})[1 - V_g^*(\lambda_g - \lambda_g z)]B_G^*(\lambda_g - \lambda_g z)}{B_G^*(\lambda_g - \lambda_g z) - z}. \quad (24) \quad 461$$

Substituting (22) and (25) into (24), we get

$$462 \quad q_{g,0} + \pi_{g,0} = \frac{1 - \rho_g}{1 - \rho_g + \lambda_g E[V_g]} \quad (25) \quad 463$$

where ρ_g is the traffic intensity of g and can be defined as
464 $\rho_g = (\lambda_g / \mu_G)$. From (17) with $k = 0$ and (26), we get
465

$$466 \quad q_{g,0} = \frac{(1 - \rho_g)V_g^*(\lambda_g)}{1 - \rho_g + \lambda_g E[V_g]} \quad (26)$$

$$467 \quad \pi_{g,0} = \frac{(1 - \rho_g)[1 - V_g^*(\lambda_g)]}{1 - \rho_g + \lambda_g E[V_g]}. \quad (27)$$

Let us assume that the service time of the controller is
468 deterministic ($\mu_c = 1/D$) and the service time of each
469 gateway exponentially distributed with a mean rate of μ_G .
470 As $V^*(x) = B^*(x)$ and $B^*(x) = e^{-Dx}$, we have $V^*(x) =$
471 $\int_0^{\infty} e^{-\lambda_g x(1-z)} dV(x) = V^*(\lambda_g - \lambda_g z)$. By substituting $(\lambda_g - \lambda_g z)$
472 in $V^*(x)$, we can obtain $V^*(\lambda_g - \lambda_g z) = e^{-D(\lambda_g - \lambda_g z)}$. From
473 the above expressions, the PGF of the number of tasks is
474 denoted as
475

$$476 \quad Q_g(z) = (q_{g,0} + \pi_{g,0}) \sum_{j=1}^K (\tau_g e^{-D(\lambda_g - \lambda_g z)})^j (1 - \tau_g). \quad (28)$$

The PGF for the number of arrivals during the service time
477 is also denoted as $A(z) = \int_0^{\infty} e^{-\lambda_g x(1-z)} dV(x) = B^*(\lambda_g -$
478 $\lambda_g z) = [\mu_G / (\mu_G + \lambda_g - \lambda_g z)]$. Thus, we have
479

$$480 \quad \Pi_g(z) = \frac{\mu_G (q_{g,0} + p_{g,0}) \left(1 - \sum_{j=1}^K (\tau_g e^{-D(\lambda_g - \lambda_g z)})^j (1 - \tau_g) \right)}{\mu_G - z(\mu_G + \lambda_g - \lambda_g z)}. \quad (29) \quad 481$$

1) *Processing Delay of the Gateway:* Once we obtain the
482 queue length, we are able to calculate the distribution of wait-
483 ing time and response time. Let W_g denote the waiting time
484 in steady state, and similarly, let $W_g^*(x)$ be the LST of W . In
485 FCFS systems, the number of jobs left after departing task is
486 equal to the number of jobs which have arrived while this task
487 was in the system, i.e., $\Pi_g(z) = W_g^*(\lambda_g - \lambda_g z)B^*(\lambda_g - \lambda_g z)$.
488 Thus, we have
489

$$490 \quad W_g^*(x) = \frac{x(1 - \rho_g)V_g^*(x)}{x - \lambda_g + \lambda_g B_G^*(x)}. \quad (30)$$

The LST of the response time of each gateway is obtained
491 by $T_g^*(x) = W_g^*(x)B_g^*(x)$ and the mean value of the response
492 time is obtained as $-T_g'(0)$. Thus, we have
493

$$494 \quad T_{p,g} = \bar{T}_g = \frac{v_g^{(2)}(1)}{2\lambda_g v_g} + \frac{\lambda_g b_G^{(2)}}{2(1 - \rho_g)} + b_G \quad (31)$$

where $v_g = -(d/ds)V_g^*(0)$, $b_G = -(d/ds)B_G^*(0)$, and $b_G^{(2)} =$
495 $-(d^2/ds^2)B_G^*(0)$.
496

497 2) *Transmission Delay of the Gateway*: We assume IoT
 498 devices are periodically sending the sensed data in exponential
 499 distribution with mean $T_s = 1/\lambda_s$. Since the data in cache
 500 have a limited validity time, a gateway checks data valid-
 501 ity upon receiving a new request from the controller. If the
 502 data are valid, it will serve the request using data in the
 503 cache, otherwise, it will fetch the fresh data from IoT devices
 504 through sending a validation GET message. As we calculate
 505 in (2), $P_{\text{OR},g}$ denote the probability of sending refresh mes-
 506 sages toward IoT devices. Thus, the transmission time can be
 507 obtained as

$$508 \quad T_{t,g} = P_{\text{OR},g} \times T_{\text{rtt}} = \frac{T_{\text{rtt}} \lambda_g e^{-(\lambda_g + \lambda_s) T_s}}{\lambda_g + \lambda_s} \quad (32)$$

509 where T_{rtt} is the round trip time at the medium access control
 510 (MAC) layer that we calculate it using the method proposed
 511 in [32]. Note that we neglect the average network delay of the
 512 SDN-based core switches in delivering the traffic to the clients.

513 E. AHP-Based Load Association Scheme

514 AHP is an effective multicriteria decision-making method
 515 that is used for finding the best case among other feasible
 516 alternatives in decision-making problems such as load
 517 management.

518 Decision making in this method is done based on a set
 519 of evaluation metrics, and through nominating convenient
 520 weights for each metrics that are derived from experts. We
 521 apply a modified AHP that is able to integrate network
 522 statistics in the ranking procedure.

523 1) *Ranking the Gateways*: Although it seems preferable to
 524 send task requests to the nearest gateways with more compu-
 525 tational resources, this may lead to an unbalanced processing
 526 load among gateways. This can affect the task's completion
 527 time, which is not suitable in delay-sensitive applications.
 528 Thus, network parameters, such as *available resources*, *link*
 529 *quality*, and *resource load* can be considered as comparison
 530 metrics in task associations to the gateways.

531 In this method, a priority is assigned to each gateway with
 532 respect to the weights of different metrics, in which these
 533 weights are defined in $1 \leq i \leq 9$, $i \in Z$ for each metric accord-
 534 ing to the AHP algorithm. The resource load can be applied
 535 as the main metric for balancing the loads among gateways
 536 since it reflects the current load status of each gateway in the
 537 network. Resource load index (LI) is defined as the remain-
 538 ing service time of the current task, in addition to the service
 539 time of the tasks that are waiting in the queue. The LST of
 540 remaining service time can be defined as

$$541 \quad B_g^+(x) = \frac{1 - B_g^*(x)}{x b_{p,x}}. \quad (33)$$

542 Thus, LI can be obtained by $L_g^*(x) = B_g^+(x)W_g^*(x)$, and
 543 $\overline{L}_g = -L_g^*(0)$.

544 Let us assume that the gateway g_1 is the overloaded gate-
 545 way, and the gateways g_2 and g_3 are the candidate overlapping
 546 gateways with g_1 . First, we calculate the preference of select-
 547 ing each gateway in a comparison matrix as in Table II, where
 548 $p_{ij} = (\overline{L}_j / \overline{L}_i)$. From the last relation, we deduce $p_{ij} = (1/p_{ji})$.

Algorithm 1 AHP-Based Load Association

```

1: Initialization:
a)  $P_k \leftarrow$  arrival task
b)  $\mathcal{G}_g \leftarrow$  overlapping gateways of  $g$ 
c)  $q_{\text{over}} = \emptyset$ , List of overloaded gateways
d)  $q_{\text{normal}} = \emptyset$ , List of normal loaded gateways
e)  $q_{\text{under}} = \emptyset$ , List of underloaded gateways
2: For  $g$  from 1 to  $m$  do
3:   If  $P_k$  is for gateway  $g$ 
4:     calculating  $T_{\text{tot},g} = T_{t,g} + T_{p,g}$ 
5:     If  $T_{\text{tot},g} > \delta_H$ 
6:       sending  $g$  into  $q_{\text{over}}$ 
7:       for all  $i$  in  $\mathcal{G}_g$  do
8:         calculating  $\overline{L}_i$  according to (31)
9:         calculating the priorities according to Table II-V
10:        selecting the most suitable  $i \in \mathcal{G}_g$ 
11:        sending  $P_k$  to gateway  $i$ 
12:      end for
13:    elseif  $\delta_L < T_{\text{tot},g}$ 
14:      sending  $g$  into  $q_{\text{under}}$ 
15:      sending  $P_k$  to  $g$ 
16:    else
17:      sending  $g$  into  $q_{\text{normal}}$ 
18:      sending  $P_k$  to  $g$ 
19:    end if
20:  end if
21: end for
  
```

TABLE II
RESOURCE LOAD COMPARISON

Resource Load	g_1	g_2	g_3
g_1	1	p_{12}	p_{13}
g_2	p_{21}	1	p_{23}
g_3	p_{31}	p_{32}	1

TABLE III
PREFERENCE MATRIX

RL	g_1	g_2	g_3
g_1	$a_{11} = \frac{1}{1+p_{21}+p_{31}}$	$a_{12} = \frac{p_{12}}{p_{12}+1+p_{32}}$	$a_{13} = \frac{p_{13}}{p_{13}+p_{23}+1}$
g_2	$a_{21} = \frac{1}{1+p_{21}+p_{31}}$	$a_{22} = \frac{1}{p_{12}+1+p_{32}}$	$a_{23} = \frac{p_{23}}{p_{13}+p_{23}+1}$
g_3	$a_{31} = \frac{p_{31}}{1+p_{21}+p_{31}}$	$a_{32} = \frac{p_{32}}{p_{12}+1+p_{32}}$	$a_{33} = \frac{1}{p_{13}+p_{23}+1}$

TABLE IV
FINAL PRIORITIES

Resource Load	g_1	g_2	g_3	priority
g_1	1	p_{12}	p_{13}	$w_1 = \frac{a_{11}+a_{12}+a_{13}}{3}$
g_2	p_{21}	1	p_{23}	$w_2 = \frac{a_{21}+a_{22}+a_{23}}{3}$
g_3	p_{31}	p_{32}	1	$w_3 = \frac{a_{31}+a_{32}+a_{33}}{3}$

To obtain the preference of the gateways, we calculate the priority of each gateway with respect to the resource load according to the AHP algorithm. The preference matrix, Table III, is obtained by dividing each element with the sum value of each column, i.e., $a_{ij} = [p_{ij}/(p_{ij} + p_{jj} + p_{kj})]$.

Finally, the priorities can be obtained by normalizing the preference matrix as $w_i = [(a_{ii} + a_{ij} + a_{ik})/3]$, shown in Table IV.

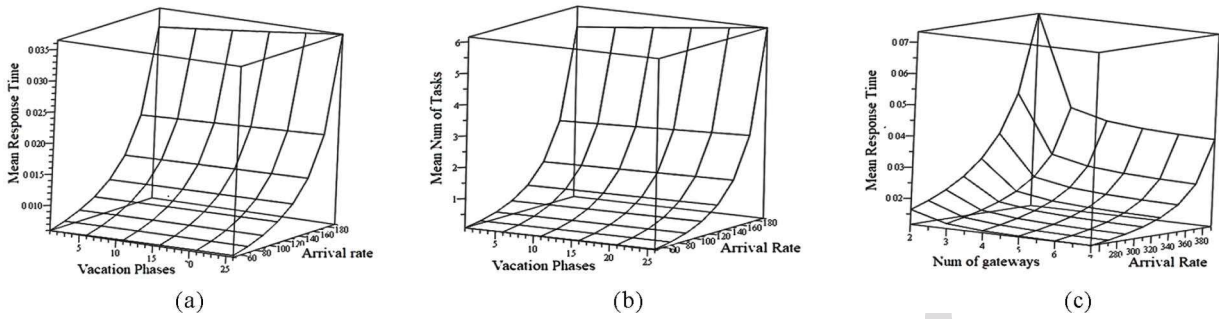


Fig. 7. Main descriptors of the IoT system with different parameters. (a) Mean response time of each gateway. (b) Mean number of tasks in each gateway. (c) Mean response time of the network.

TABLE V
RESOURCE LOAD COMPARISON & PRIORITY

Resource Load	g_1	g_2	g_3	priority
g_1	1	0.6	0.5	0.22
g_2	1.48	1	0.7	0.33
g_3	1.87	1.25	1	0.44

Let us assume that LI of the three gateways are calculated as $L_1 = 2.61$ ms, $L_2 = 1.75$ ms, and $L_3 = 1.39$ ms, respectively. Thus, the comparison matrix for these three gateways is obtained as Table V.

After calculating the priorities of each gateway with respect to the preferred metrics, the convenient gateway can be selected based on these priorities. To ensure the consistency of prioritization in metric weights, the consistency ratio (CR) can be calculated to check the degree of consistency, which should be $CR \leq 0.1$ [21]. The details of the MCDM-based load-balancing algorithm is shown in the following pseudocode. As seen, the calculations are done for each of the overlapping ping gateways in the network, and the number of overlapping gateways is limited ($2 < m < 4$). The overall computational complexity of computing the exact stationary queue length distribution is $O(K^2)$ [33], where K is the buffer size. Note that in our algorithm, the buffer size cannot be infinite due to the upper threshold (δ_H) for the server load. On the other hand, time complexity of AHP is in $O(\min\{mn^2, m^2n\})$ time, where m is candidates and n is metrics [34]. Thus, the total complexity is $O(K^2) + O(\min\{mn^2, m^2n\})$.

IV. PERFORMANCE EVALUATION

To evaluate the performance of the load-balancing model, we consider a single-hop 6LoWPAN-based WSN with multiple overlapping gateways. The analytical model has been solved using Maple 16 from Maplesoft, Inc., [35] and MATLAB is used to run different simulation scenarios. The performance of the network is analyzed in a number of different scenarios.

In the first step, we evaluate the analytical model with different parameters, such as task arrival rate and different vacation phases. Fig. 7 illustrates the effect of queuing parameters on the performance measures of the model. In the first scenario, we have considered multivacation-based queueing model with different arrival ratio, varying from $\lambda_g = 0.2\lambda$ to $\lambda_g = 0.8\lambda$

task arrival per second to an arbitrary gateway ($\lambda = 250$ arrivals per second). To investigate the effect of the number of phases of vacation on the system performance, we assumed each gateway can take different vacation phases from $K = 1$ to $K = 30$ in each iteration. The execution time of each gateway is exponentially distributed and the average gateway execution time is set to $(1/\mu_G) = 45$ ms.

The mean response time for each gateway g is shown in Fig. 7(a). As it is observed from the figure, increasing the number of vacation phases induces a higher level of response time for the gateway. However, the delay imposed by the vacation period is more noticeable in the higher arrival rate. Because in higher rates of task arrival, the length of vacation period taken by the gateways is longer than lower rates.

Fig. 7(b) shows the number of tasks waiting in the queue for each gateway. As can be seen, the mean number of tasks is increasing function with respect to both request arrival rate and the number of phases of vacation. However, when $\lambda_g = 200$, the graph rises with a steep slope as compared to $\lambda_g = 50$. The reason for this is due to the fact that when the task arrival rate increases, the probability of taking longer vacation periods rises for each gateway. Thus, the graph rises with the steeper rate in higher arrival rates.

In the next step, we consider the end-to-end delay of the network in different scenarios. First, the average delay of the SDN-based IoT domain is considered with different arrivals from $\lambda = 250$ to $\lambda = 400$, and varying number of gateways (from 2 to 7) in the system. The maximum vacation phases is set to $K = 30$, and the average execution time of the gateways is considered $1/\mu_G = 45$ ms, respectively. Fig. 7(c) shows that the average delay of the tasks increases with the number of gateways whilst it shows a small rise with arrival rate. The reason for this is the contention of additional gateways on the controller and longer vacation periods that are induced for each gateway.

The next scenario evaluates the effectiveness of MCDM-based load balancing in comparison with the conventional round robin (RR) and response time-based load-balancing method [26]. RR load balancing is a way that widely used to distribute client requests among the servers due to its simplicity. As known in RR, the requests are forwarded to each server in turn and the algorithm instructs the load balancer to jump back to the beginning of the list once the end is reached

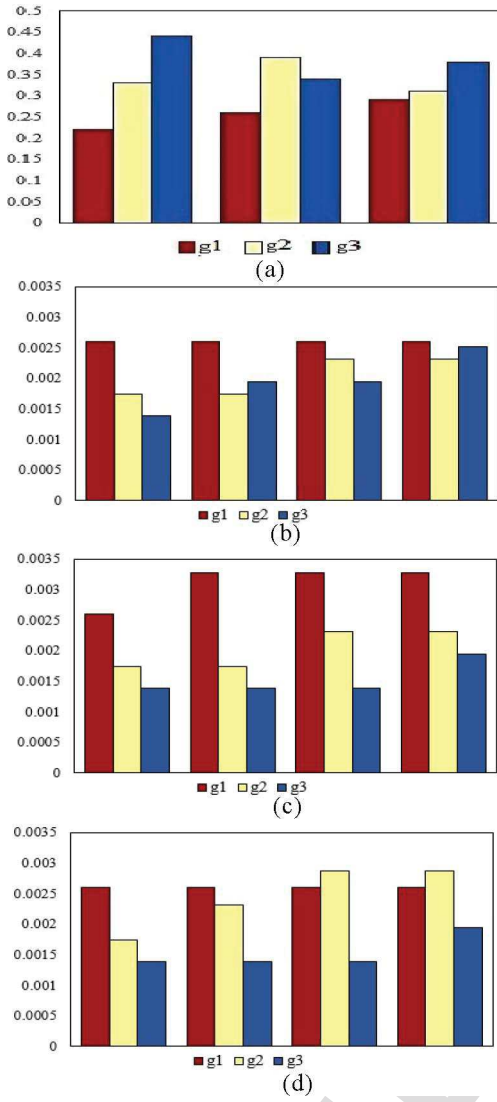


Fig. 8. (a) Priority of gateways over time. (b) Loads in MCDM-based method. (c) Loads in RR method. (d) Loads in LBBSRT.

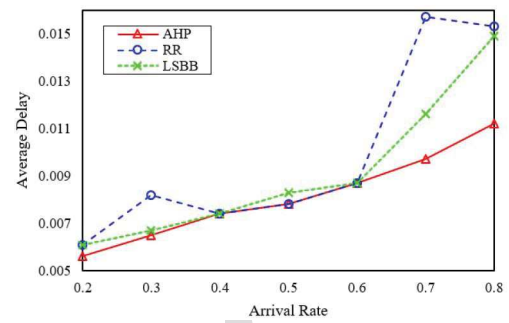


Fig. 9. Network latency in three methods.

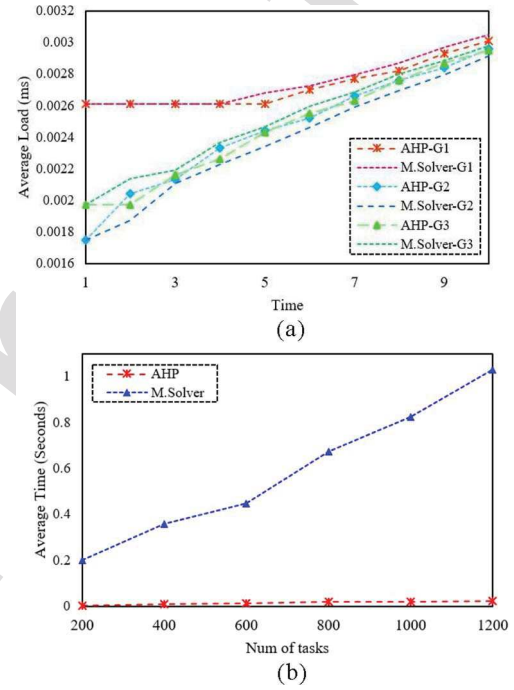


Fig. 10. (a) Average load of gateways. (b) Average execution time.

and repeats again. This solution can achieve a better response time than a random load-balancing strategy [28]. However, considering the server delay in traffic load balancing can help to obtain better response time. In addition, server load may impact on selecting the appropriate threshold for the response times. So, we take into account the weighted index of network features in balancing the traffic loads.

In order to evaluate it, a domain with three overlapping gateway ways are considered with LI of $L_1 = 2.61$ ms, $L_2 = 1.75$ ms, and $L_3 = 1.39$ ms for each gateway. Fig. 8(a) illustrates the variation of the gateways priority with respect to their Resource LI. As can be seen, the priority of the gateways almost converges to the same value over time as the load is assigned to them in a fairly manner. Fig. 8(b)–(d) demonstrates the comparative results of the LI of the gateways in three methods. The graphs clearly depict that the proposed method evenly dispatches the loads among the gateways, while other methods lead to the partly unfair load association among resources.

To investigate the performance of the network in three methods, the average delay of task execution for three gateways

is calculated with the arrival task rate in Fig. 9. The figure shows the variable delay experienced by gateways in the RR method due to the unbalanced allocations of the requests by the arrival rate. As expected, the average delay increases with the arrival rate for all approaches. However, this rate rises with a steep slope for the RR method as compared to two other methods. This graph clearly shows the effectiveness of the MCDM-based load-balancing approach as compared to RR and LBBSRT in providing a fast response to the user queries.

In the next experiment, we evaluate the performance of the MILP version and the AHP algorithm in terms of the average load of gateways [Fig. 10(a)] and average execution time [Fig. 10(b)]. As the graphs illustrate, the average load of the gateways is almost the same in both approaches. However, by increasing the number of tasks, the average execution time of the MILP-based model shows a notable growth due to the time complexity issue, while the AHP algorithm determines a reasonable solution for all cases of task number.

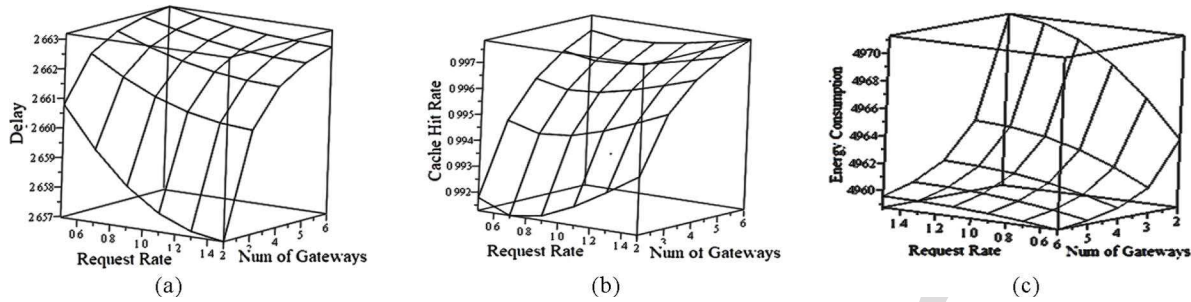


Fig. 11. Main descriptors of the system when number of the gateways varies between 2 and 6, maximum allowed phases of vacation is 30, λ varies between 0.5 and 0.15 arrivals per minute, and service rate of the gateways $\mu_G = 220$, respectively. (a) End-to-end delay in network. (b) Probability of cache hit in a gateway. (c) Energy consumption of network.

676 A. Performance of the Combined Load-Balancing and 677 Caching Strategy

678 In this section, we evaluate the performance of the proposed
679 model over IEEE 802.15.4, the total number of IoT devices is
680 set to 200 sensor nodes. We assumed the packet size of 127 B
681 with a bit error rate of $BER = 10^{-5}$. The Poisson arrival rate of
682 requests is varied from 0.5 to 1.5 arrivals per minute, and the
683 average service time of the gateways is 22 ms. Fig. 11 shows
684 the performance measure of the network. We noted that the
685 end-to-end delay of the network increases with the number
686 of the gateways. The reason for this is the increased vacation
687 periods induced to the proxies in a higher number of the gate-
688 ways. However, this parameter falls with the request arrival
689 rate as incoming tasks benefit from the updating work by val-
690 idations triggered by queries from previous tasks. As a result,
691 the cache hit rate increases with a higher rate of user queries.
692

693 Fig. 11(b) illustrates the combined effect of the gateways
694 and the arrival rate in the proxy cache hit rate. As noted,
695 the cache hit rate is increased by rising the number of gate-
696 ways. However, this rate shows a mild decrease with the user
697 request rate in the beginning due to the increased amount of
698 outdated entries in the cache. Then, it begins to increase as the
699 new arrival requests benefits from the updated data cached by
700 the queries from previous tasks. As mentioned previously, the
701 network latency consists of processing delay and transmission
702 delay. So, the increased ratio of cache miss will lead to the
703 increased latency of the network. This, in turn, can impact on
704 the energy consumption of the sensor nodes.

705 The energy consumption per node, shown in Fig. 11(c),
706 is decreased by increasing the number of gateways. Again,
707 the impact of the user request rate is visible in increasing
708 the energy consumption per node. Thus, an appropriate load
709 association scheme can lead to save the energy of IoT devices.
710 Finally, we note that energy consumption can decrease with
711 increasing the number of gateways as it distributes the traffic
712 loads among the gateways and accordingly reduces the cache
713 miss rate and recaching operations in the gateways.

714 As seen from the results, the proposed multigateways archi-
715 tecture along with a resource caching policy can provide fast
716 responses and reduced energy consumption for IoT devices.
717 Furthermore, AHP-based load balancing can help to achieve
718 a global load fairness among the network entities taking into
719 account their load changes over time. Considering a general

vacation queueing model in the evaluation and the IPv6 719
720 protocol stack over sensor devices in implementation makes 720
the evaluation closer to the real-world models. However, a 721
722 preferential treatment for different traffic flows with variable 722
723 evaluation metrics in AHP can also be applied to improve the 723
Quality of Experience (QoE) for different IoT applications. 724

V. CONCLUSION

In this article, we have proposed and analyzed the multiple 726
vacation-based queuing system to model the performance of 727
the IoT edge network. In order to speed up the user's access 728
to the sensor data, we leveraged a multigateways architecture 729
along with a resource caching policy in the IoT domain. An 730
MCDM-based load-balancing technique is also employed to 731
provide a global load fairness among the network entities. The 732
proposed model facilitates the remote access from the Internet 733
to IPv6 IoT devices by leveraging the multigateway architec- 734
ture over IEEE 802.15.4 connectivity. The evaluation results 735
show the effectiveness of the proposed solution in the fast and 736
reliable acquisition of big data from the IoT domain, which 737
is promising to drive IoT development. In future work, we 738
plan to address the scenario in which the network has differ- 739
ent traffic classes of task request which are associated to the 740
gateways according to their QoS requirements. 741

REFERENCES

- [1] J. Lin, W. Yu, N. Zhang, X. Yang, H. Zhang, and W. Zhao, "A survey on Internet of Things: Architecture, enabling technologies, security and privacy, and applications," *IEEE Internet Things J.*, vol. 4, no. 5, pp. 1125–1142, Oct. 2017.
- [2] L. Atzori, A. Iera, and G. Morabito, "The Internet of Things: A survey," *Comput. Netw.*, vol. 54, no. 15, pp. 2787–2805, 2010.
- [3] G. Xu, W. Yu, D. Griffith, N. Golmie, and P. Moulema, "Toward Integrated distributed energy resources and storage devices in smart grid: Modeling, analysis, and evaluation," *IEEE Internet Things J.*, vol. 4, no. 1, pp. 192–204, Feb. 2017.
- [4] S. Hong *et al.*, "SNAIL: An IP-based wireless sensor network approach toward the Internet of Things," *IEEE Wireless Commun.*, vol. 17, no. 6, pp. 34–42, Dec. 2010.
- [5] A. Yousefpour, G. Ishigaki, R. Gour, and J. P. Jue, "On reducing IoT service delay via fog offloading," *IEEE Internet Things J.*, vol. 5, no. 1, pp. 998–1010, Jan. 2018.
- [6] G. Montenegro, N. Kushalnagar, J. Hui, and D. Culler, "Transmission of IPv6 packets over IEEE 802.15.4 networks," Internet Eng. Task Force, RFC 4944, Sep. 2007.
- [7] T. Winter *et al.*, "RPL: IPv6 routing protocol for low-power and lossy networks," IETF, RFC 6550, 2012.

- 764 [8] Z. Shelby, K. Hartke, and C. Bormann. (Jun. 2014). *Constrained*
 765 *Application Protocol (CoAP)*, *Internet Draft*, [Online]. Available:
 766 <http://datatracker.ietf.org/wg/core/charter>
- 767 [9] Z. Sheng, H. Wang, C. Yin, X. Hu, S. Yang, and V. C. M. Leung,
 768 “Lightweight management of resource constrained sensor devices in
 769 Internet-of-Things,” *IEEE Internet Things J.*, vol. 2, no. 5, pp. 402–411,
 770 Oct. 2015.
- 771 [10] M. Kovatsch, S. Duquennoy, and A. Dunkels, “A low-PoWer CoAP for
 772 Contiki,” in *Proc. IEEE 8th Int. Conf. Mobile Ad Hoc Sensor Syst.*,
 773 Oct. 2011, pp. 855–860.
- 774 [11] T. Suganuma, T. Oide, S. Kitagami, K. Sugawara, and N. Shiratori,
 775 “Multiagent-based flexible edge computing architecture for IoT,” *IEEE Netw.*,
 776 vol. 32, no. 1, pp. 16–23, Jan./Feb. 2018.
- 777 [12] M. Armbrust *et al.*, “A view of cloud computing,” *Commun. ACM*,
 778 vol. 53, no. 4, pp. 50–58, 2010.
- 779 [13] L. Wang and R. Ranjan, “Processing distributed Internet of Things
 780 data in clouds,” *IEEE Cloud Comput.*, vol. 2, no. 1, pp. 76–80,
 781 Jan./Feb. 2015.
- 782 [14] S. Arshad, M. A. Azam, M. H. Rehmani, and J. Loo, “Recent advances
 783 in information-centric networking based Internet of Things (ICN-IoT),”
 784 *IEEE Internet Things J.*, vol. 6 no. 2, pp. 2128–2158, Apr. 2019.
- 785 [15] X. Chen, Q. Shi, L. Yang, and J. Xu, “ThriftyEdge: Resource efficient
 786 edge computing for intelligent IoT applications,” *IEEE Netw.*, vol. 32,
 787 no. 1, pp. 61–65, Jan./Feb. 2018.
- 788 [16] X. Sun and N. Ansari, “Traffic load balancing among brokers at the IoT
 789 application layer,” *IEEE Trans. Netw. Service Manag.*, vol. 15, no. 1,
 790 pp. 489–502, Mar. 2018.
- 791 [17] Q. Fan and N. Ansari, “Workload allocation in hierarchical cloudlet
 792 networks,” *IEEE Commun. Lett.*, vol. 22, no. 4, pp. 820–823, Feb. 2018.
- 793 [18] Q. Fan and N. Ansari, “Application aware workload allocation for
 794 edge computing-based IoT,” *IEEE Internet Things J.*, vol. 5, no. 3,
 795 pp. 2146–2153, Jun. 2018.
- 796 [19] Q. Fan and N. Ansari, “Towards workload balancing in fog computing
 797 empowered IoT,” *IEEE Trans. Netw. Sci. Eng.*, vol. 7, no. 1,
 798 pp. 253–262, Jun. 2018.
- 799 [20] G. Grimmett and D. Stirzaker, *Probability and Random Processes*, 3rd
 800 ed. Oxford, U.K.: Oxford Univ. Press, Jul. 2010.
- 801 [21] T. L. Satty, “Decision making with the analytic hierarchy process,”
 802 *Service Sci.*, vol. 1, no. 1, pp. 83–98, 2008.
- 803 [22] Z. Gao, X. Li, H. Zhang, and V. C. M. Leung, “A load balance self-
 804 healing algorithm based on AHP for backhaul transmission in UDNs,”
 805 in *Proc. Netw. Infrast. Digit. Content (IC-NIDC)*, 2018, pp. 315–319.
- 806 [23] A. M. Abdullah, H. A. Ali, and A. Y. Haikal, “A reliable TOPSIS-based
 807 multi-criteria and hierarchical load balancing method for computational
 808 grid,” *Clust. Comput.*, vol. 22, pp. 1085–1106, Jan. 2019.
- 809 [24] A. Lara, A. Kolasani, and B. Ramamurthy, “Network innovation using
 810 OpenFlow: A survey,” *IEEE Commun. Survey Tuts.*, vol. 16, no. 1,
 811 pp. 483–512, 1st Quart., 2014.
- 812 [25] W. Wang, S. De, R. Toenjes, E. Reetz, and K. Moessner, “A comprehensive
 813 ontology for knowledge representation in the Internet of Things,”
 814 in *Proc. 11th Int. Conf. Trust Security Privacy Comput. Commun. (TrustCom)*,
 815 2012, pp. 1793–1798.
- 816 [26] J. Cui, Q. Lu, H. Zhong, M. Tian, and L. Liu, “A load-balancing mechanism
 817 for distributed SDN control plane using response time,” *IEEE Trans. Netw. Service Manag.*,
 818 vol. 15, no. 4, pp. 1197–1206, Dec. 2018.
- 819 [27] C. Cotta and J. M. Troya, “A hybrid genetic algorithm for the 0–1
 820 multiple knapsack problem,” in *Artificial Neural Nets and Genetic
 821 Algorithms*. Heidelberg, Germany: Springer, 1998, pp. 250–254.
- 822 [28] S. Kaur, K. Kumar, J. Singh, and N. S. Ghuman, “Round-robin based
 823 load balancing in software defined networking,” in *Proc. Int. Conf.
 824 Comput. Sustain. Global Develop. (INDIACOM)*, 2015, pp. 2136–2139.
- 825 [29] J. Misic, V. B. Misic, and F. Banaie, “Reliable and scalable data acquisition
 826 from IoT domains,” in *Proc. IEEE GlobeCom*, Singapore, 2017,
 827 pp. 1–6.
- 828 [30] H. Takagi, *Queueing Analysis: Vacation and Priority Systems*, vol. 1.
 829 Amsterdam, The Netherlands: North-Holland, 1991.
- 830 [31] N. Tian and Z. Zhang, *Vacation Queueing Models: Theory and
 831 Applications*. Berlin, Germany: Springer, 2006.
- 832 [32] J. Misic and V. B. Misic, *Wireless Personal Area Networks:
 833 Performance, Interconnections and Security With IEEE 802.15.4*.
 834 Hoboken, NJ, USA: Wiley, 2008.
- 835 [33] H. Li and Y. Zhu, “M(n)/G/1/N queues with generalized vacations,”
 836 *Comput. Oper. Res.*, vol. 24, no. 4, pp. 301–316, 1997.
- 837 [34] N. Z. Mamat and J. K. Daniel, “Statistical analyses on time complexity
 838 and rank consistency between singular value decomposition and the
 839 duality approach in AHP: A case study of faculty member selection,”
 840 *Math. Comput. Model.*, vol. 46, no. 7, pp. 1099–1106, 2007.
- [35] (2015). *Maplesoft, Maple 16*. [Online]. Available: <http://www.maplesoft.com/products/maple>
- 841
 842
 843
 844
 845
 846
 847
 848
 849
 850
 851
 852
 853
 854
- Fatemeh Banaie** (Student Member, IEEE) received the M.Sc. degree in software computer engineering from the Ferdowsi University of Mashhad, Mashhad, Iran, in 2012, where she is currently pursuing the Ph.D. degree with the Computer Engineering Department.
- From November 2016 to November 2017, she was a Visiting Research Scholar with the Department of Computer Science, Ryerson University, Toronto, ON, Canada. Her research interests are in the area of cloud networking, resource management, and Internet of Things.
- Mohammad Hossein Yaghmaee** (Senior Member, IEEE) is a Full Professor with the Computer Engineering Department, Ferdowsi University of Mashhad, Mashhad, Iran. From November 1998 to July 1999, he was a Visiting Research Scholar with the Network Technology Group, C&C Media Research Laboratories, NEC Corporation, Tokyo, Japan. From September 2007 to August 2008, he was a Visiting Associate Professor with the Lane Department of Computer Science and Electrical Engineering, West Virginia University, Morgantown, WV, USA. From July 2015 to September 2016, he was a Visiting Professor with the Electrical and Computer Engineering Department, University of Toronto, Toronto, ON, Canada. His research interests are in smart grid communication, software-defined networking, and network function virtualization.
- Seyed Amin Hosseini** received the B.Sc. and M.Sc. degrees in computer engineering from the Ferdowsi University of Mashhad, Mashhad, Iran, in 1990 and 1998, respectively, and the Ph.D. degree in computer network from the University of Science, Malaysia, in 2010. He is the Dean of the Information and Communication Center, Ferdowsi University of Mashhad. His research interests include wireless networks, energy efficiency protocols, and network security.
- Farzad Tashtarian** is an Assistant Professor with the Department of Computer Engineering and the Head of the System and Computer Networking Research Center, Islamic Azad University of Mashhad, Mashhad, Iran. He is also a Member of the Young Researchers and Elite Club, Mashhad Branch, Islamic Azad University. From February 2013 to October 2013, he was a Visiting Scholar with the University of Missouri Kansas City, Kansas City, MO, USA. He has coauthored several research papers and published in well-known conferences and journals, including IEEE Global Communications Conference, IEEE/ACM International Symposium on Quality of Service, the IEEE TRANSACTIONS ON VEHICULAR TECHNOLOGY, the IEEE TRANSACTIONS ON NETWORK AND SERVICE MANAGEMENT, and Future Generation Computer Systems (Elsevier). He is broadly interested in software-defined networking, network function virtualization, multimedia streaming, Internet of Vehicles, mathematical modeling, and distributed optimization.